

# Investigation of the mechanism of enhanced and directed differentiation of neural stem cells by an atmospheric plasma jet: A gene-level study

Cite as: J. Appl. Phys. **125**, 163301 (2019); <https://doi.org/10.1063/1.5060650>

Submitted: 21 September 2018 . Accepted: 01 April 2019 . Published Online: 22 April 2019

Shasha Zhao, Rui Han, Yuan Li, Chen Lu, Xingyu Chen, Zilan Xiong , and Xiang Mao



View Online



Export Citation



CrossMark

## ARTICLES YOU MAY BE INTERESTED IN

[Comparative study on diffuse dielectric barrier discharges excited by unipolar positive versus bipolar pulses in atmospheric air](#)

Journal of Applied Physics **125**, 163304 (2019); <https://doi.org/10.1063/1.5085456>

[Cold atmospheric helium plasma jet in humid air environment](#)

Journal of Applied Physics **125**, 153301 (2019); <https://doi.org/10.1063/1.5086177>

[Diagnosing the lightning plasma temperature based on the collisional-radiative model](#)

Journal of Applied Physics **125**, 163305 (2019); <https://doi.org/10.1063/1.5087739>

Journal of  
Applied Physics

SPECIAL TOPIC:  
Polymer-Grafted Nanoparticles

Submit Today!

# Investigation of the mechanism of enhanced and directed differentiation of neural stem cells by an atmospheric plasma jet: A gene-level study

Cite as: J. Appl. Phys. **125**, 163301 (2019); doi: [10.1063/1.5060650](https://doi.org/10.1063/1.5060650)

Submitted: 21 September 2018 · Accepted: 1 April 2019 ·

Published Online: 22 April 2019



Shasha Zhao,<sup>1</sup> Rui Han,<sup>2</sup> Yuan Li,<sup>1</sup> Chen Lu,<sup>2</sup> Xingyu Chen,<sup>2</sup> Zilan Xiong,<sup>2,a)</sup>  and Xiang Mao<sup>3</sup>

## AFFILIATIONS

<sup>1</sup>College of Life Science and Health, Wuhan University of Science and Technology, Wuhan, People's Republic of China

<sup>2</sup>State Key Laboratory of Advanced Electromagnetic Engineering and Technology, Huazhong University of Science and Technology, Wuhan, Hubei, People's Republic of China

<sup>3</sup>Wuhan Centers for Disease Prevention and Control, 24 Jiangnan N. Road, Wuhan, Hubei, People's Republic of China

<sup>a)</sup>E-mail: [zilanxiong@hust.edu.cn](mailto:zilanxiong@hust.edu.cn).

## ABSTRACT

Cold atmospheric plasmas (CAPs) have been shown to be capable of enhancing stem cell differentiation, especially directed differentiation of neural stem cells (NSCs). Consequently, one-step CAP treatment shows promise as an aid to tissue transplantation. However, the mechanisms involved in the enhancement of NSCs differentiation by CAP treatment are not yet fully understood. We have previously shown that in atmospheric helium plasma jet treatment, nitric oxide (NO) is the main factor involved in promoting NSC differentiation. This article further investigated the possible signaling pathways stimulated by NO in the neuronal differentiation of C17.2-NSCs after plasma treatment. Extracellular and intracellular NO concentrations were measured at different time points of incubation to monitor NO production. Meanwhile, the expressions of related genes and proteins were detected by quantitative real-time polymerase chain reaction and western blot, respectively. It is found that plasma treatment could both generate extracellular NO and increase extracellular NO concentration by inducing inducible nitric oxide synthase expression. The synergetic effect of extracellular and intracellular NO then downregulated Notch1 and Id2, and upregulated Ngn2 and Ascl1, thereby activating downstream NeuroD expression and finally enhancing and directing differentiation of NSCs into neurons.

Published under license by AIP Publishing. <https://doi.org/10.1063/1.5060650>

## I. INTRODUCTION

Neurological diseases and disorders, particularly those that affect the brain, such as Alzheimer's disease and other dementias, Parkinson's disease, and brain tumors, occur more commonly in elderly people and are found to be the largest cause of disability worldwide.<sup>1</sup> According to a Global Burden of Disease Study, the population with neurological diseases has recently grown substantially, with the number of deaths from neurological disorders increasing by 36.7% between 1990 and 2015, and this burden will continue to increase as the global population continues to age.<sup>2</sup> In addition to drug treatment, surgery, and gene therapy, the use of neural stem cells (NSCs) in tissue engineering represents one of the most promising approaches to the treatment of neurodegenerative and neurotraumatic diseases.

NSCs are able to differentiate into neurons, oligodendrocytes, and astrocytes *in vitro* under certain conditions. It has been shown that a number of growth factors and other biological molecules, as well as electrical stimulation and the microenvironment, have significant effects on NSC differentiation.<sup>3,4</sup> For example, insulin may act as a myogenic differentiation signal for NSCs,<sup>5</sup> seeding on three-dimensional collagen gel scaffolds can increase the differentiation potential of NSCs,<sup>6</sup> and the application of a pulsed electrical current to poly(3,4-ethylenedioxythiophene) doped with poly(styrene sulfonic acid) (PEDOT:PSS) can elongate both NSCs and neurons.<sup>7</sup> However, none of these methods could precisely control and enhance cell fate commitment or differentiation into a desired cell lineage. In addition, chemical toxicity, scar formation, and other deleterious side effects have

limited the clinical application of NSCs to tissue engineering and regeneration.

Neurons are the core components of the brain, spinal cord, and peripheral nervous system, and so the direct differentiation of NSCs into neurons is of great importance for cell-based nerve regeneration strategies. For example, Parkinson's disease is characterized by loss of A9 nigral dopamine neurons, and clinical trials of cell transplantation have already been performed for this prototypic neurodegenerative condition.<sup>8</sup> The differentiation of NSCs into neurons is a coordinated response which is regulated by many genes,<sup>9</sup> such as the *Tlx* gene, the *Sox* gene family, the basic helix-loop-helix (bHLH) family, and the *Pax* gene family. *Tlx* is expressed in sensory neurons and postsynaptic neurons in central relay stations, and its expression determines neuronal connectivity.<sup>10</sup> The *Sox* gene family plays a role in maintaining the undifferentiated state of NSCs, and *Sox2* is not expressed in layers where differentiated neurons are present.<sup>11</sup> The bHLH family is reported to play a critical role in the maintenance and differentiation process of NSCs.<sup>12</sup> *Pax6* is expressed in immature neurons.<sup>13</sup>

Nitric oxide (NO) is a short-lived, highly reactive gas that serves as a gaseous chemical messenger in biological systems and participates in various physiological processes. It can be synthesized inside the cell by reaction of O<sub>2</sub> and L-arginine under enzymatic catalysis by three isotypes of NO synthase (NOS).<sup>14</sup> NO also acts as a neurotransmitter in the brain and plays possible roles in the regulation of progenitor cell proliferation, differentiation, and migration in brain development. Zhang *et al.*<sup>15</sup> found that NO is involved in the regulation of progenitor cells and that injection of the NO donor diethylenetriamine (DETA) NONOate could induce neurogenesis and reduce functional deficits after stroke in rats. NO also acts as an amplifier of calcium signals in neuronal cells,<sup>16</sup> and intracellular increases in Ca<sup>2+</sup> may protect neurons from developmental cell death.<sup>17</sup>

Cold atmospheric plasma (CAP) is an ionized gas containing reactive oxygen/nitrogen species (RONS) with a gas temperature which could close to room temperature and is a potentially useful tool for various biomedical applications, including, among others, cancer treatment, enhancement of cell proliferation and stem cell differentiation, decontamination, skin wound treatment, and root canal treatment in dentistry.<sup>18–24</sup> In recent years, a number of clinical trials of CAP treatment have been reported, and several CAP devices are now commercially available.<sup>25–28</sup> It has been shown that effective generation of gaseous NO from a CAP is possible using a range of plasma source designs. The concentration of RONS created in the plasma depends mainly on the nature of the working gas mixture and the input power. In a surface microdischarge (SMD), as the input power is increased, three production modes appear: the O<sub>3</sub> mode, the transient mode, and the NOx mode. Pavlovich *et al.*<sup>29</sup> found a quantitative relationship between these three modes, and ozone is produced at low power density; at high enough power density, above approximately 0.10 Wcm<sup>-2</sup>, the gaseous chemistry will eventually transit from an ozone-producing mode to a nitrogen oxides-producing mode; and at high power density above ~0.4 Wcm<sup>-2</sup>, the NOx production will dominate the gaseous chemistry. Douat *et al.*<sup>30</sup> studied the production of nitric and nitrous oxides by an atmospheric-pressure plasma jet (APPJ) and found that the production regime depends on the power, flow, and gas mixture. Pipa *et al.*<sup>31</sup> also performed an experiment on controlling the NO production in an APPJ and concluded that the NO radicals could be

controlled by variation of the air content in an Ar/air mixture. From these results, it, therefore, appears that CAP may serve as a viable and controllable NO source for application to neuronal differentiation.

In our previous work, we found that a cold helium/oxygen atmospheric plasma jet was able to induce differentiation of both the murine immortalized neural stem cell line C17.2 (C17.2 NSCs) and primary rat neural stem cells *in vitro*.<sup>32</sup> By using the NO donor sodium nitroprusside (SNP) as a positive control and the NO scavenger hemoglobin (Hgb) as a negative control, it was found that NO played a dominant role in the differentiation process. A recent study by Jang *et al.*<sup>33</sup> used a dielectric barrier discharge (DBD) device to accelerate the differentiation of mouse neuroblastoma Neuro 2A (N2a) cells, thus confirming our results, and even to realize the promotion of neural maturation in zebrafish *in vivo*. They claimed that NO served as an upstream extracellular messenger that played a critical role in communicating with cells during CAP-induced neural differentiation. However, studies on the application of CAPs to NSCs differentiation are limited, and the mechanisms by which CAPs enhance this differentiation are far from understood. Hence, the present investigation focuses mainly on how the NO generated by an atmospheric plasma jet enhances selective and directed differentiation of C17.2 NSCs into neurons, in particular, through gene regulation and signaling protein expression.

## II. EXPERIMENTAL PREPARATION AND METHODS

### A. Cell culture

The murine immortalized NSC line C17.2 (C17.2 NSC) was used in this investigation and maintained in Dulbecco's modified Eagle's medium (DMEM, Gibco BRL, Grand Island, NY) with 10% fetal bovine serum (FBS), 5% horse serum (HS), and 1% penicillin/streptomycin (Hyclone, Logan, UT) as supplements in a humidified atmosphere of 5% CO<sub>2</sub> and 95% air at 37 °C. Cells in the logarithmic phase were detached by trypsin and planted onto a 12-well plate with a cell density of ~2 × 10<sup>4</sup> cells/well. After attachment, cells were washed twice with serum-free DMEM and cultured in differentiation medium containing DMEM/F-12 (Hyclone, Logan, UT) with 1% N-2 supplement (Gibco BRL, Grand Island, NY) for 48 h prior to plasma treatment. Controls were kept in differentiation medium at room temperature during the experimental procedures.

### B. Low-temperature atmospheric plasma jet device and *in vitro* plasma treatment

A single-electrode atmospheric low-temperature plasma jet device was used, as shown in Fig. 1, where (a) is an overview of the whole system and (b) is a three-dimensional sketch of the plasma jet source. A high-voltage wire in a quartz tube sealed at one end, acting as a high-voltage electrode, was inserted into a syringe. A holder with holes was mounted in the center of the syringe for fixation of the high-voltage electrode and to supply a gas flow. The high-voltage wire was connected to a pulsed DC power supply with fixed output (8 kV, 1600 ns, and 8 kHz). A high-voltage probe (Tektronix P6015A) and oscilloscope (Tektronix DPO3034) were used to detect the output voltage. The working gases (helium plus 1% O<sub>2</sub>) were fed under the control of a mass flow controller (MKS,

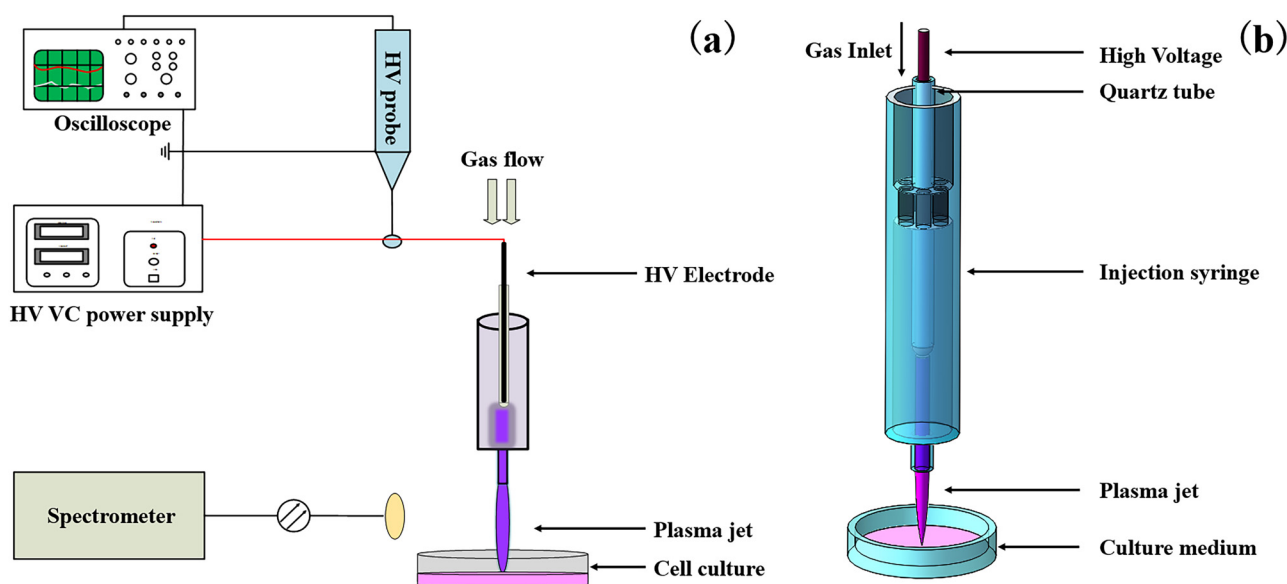


FIG. 1. (a) Sketch of the experimental setup. (b) Structure of the He/O<sub>2</sub> plasma jet device.

USA). The distance between the syringe tip and the surface of the cell culture medium was fixed at 15 mm for all treatments. More details of the plasma jet device can be found in Ref. 34.

Before treatment, the medium of the predifferentiated cells was replaced with 800  $\mu$ l of fresh differentiation medium. Then, samples were randomly divided into three groups: control, gas flow control, and plasma-treated. The control and gas flow control groups refer, respectively, to untreated cells and cells treated by gas flow alone with the plasma off. After plasma treatment, 1 ml new differentiation medium was added to each hole to replace the original culture medium. The samples were then incubated in a humidified atmosphere of 5% CO<sub>2</sub> and 95% air at 37 °C.

### C. Immunofluorescence and cell morphology observation

In preparation for immunofluorescence analysis, cells were seeded on PDL-coated coverslips with a diameter of 20 mm (Sigma Chemical Co., St. Louis, MO). The cell culture preparation was described in Sec. II A. After plasma treatment and incubation, the samples were fixed with 4% paraformaldehyde (Beyotime, Jiangsu, China) for 20 min at room temperature and then permeabilized with 0.2% Triton X-100 for 10 min. Next, the cells were washed three times with phosphate-buffered saline (PBS) and incubated with 10% goat serum for 1 h to block any nonspecific interactions. The samples were then incubated with  $\beta$ -Tubulin III antibody (Sigma Aldrich, USA) at 4 °C overnight. The cells were further incubated with Cy3-conjugated secondary antibody (Jackson Immuno Research, USA) for 1 h at room temperature after being washed with PBS. Hoechst 33258 (Beyotime, Jiangsu, China) was used to label nuclei. A Nikon fluorescence microscope (80i, Nikon, Tokyo, Japan) was used to image specific protein expressions.

General cell morphology was recorded by an inverted phase contrast light microscope (XD-202, Nanjing Jiangnan Novel Optics Co., Ltd) and photographs were taken every day for morphological analysis.

### D. Quantitative RT-PCR

Total RNA was extracted with the RNeasy pure cell/bacteria kit (Qiagen Biotech, Beijing, China). Approximately 1.5  $\mu$ g RNA from each sample was reverse transcribed into cDNA and subsequently served as the template for quantitative real-time polymerase chain reaction (qRT-PCR) using a RevertAid first-strand cDNA synthesis kit (Fermentas, USA). The primers of the target genes are listed in Table I, and qRT-PCR was performed on a Bio-Rad CFX-96 detection system (Bio-Rad, Hercules, CA). The reaction mixture contained 10  $\mu$ l SuperReal Premix Plus (2 $\times$ ) (Tiangen Biotech), 1.2  $\mu$ l of a 10  $\mu$ M solution of sense/antisense primers, 1  $\mu$ l template DNA, and 7.8  $\mu$ l ddH<sub>2</sub>O. The qRT-PCR program consisted of one cycle of 95 °C for 15 min, and then 40 cycles of 95 °C for 10 s, 60 °C for 20 s, and 72 °C for 20 s. At the completion of each run, melting curves from 65 °C to 94 °C were monitored to assess the dissociation characteristics of double-stranded DNA product. Glyceraldehyde 3-phosphate dehydrogenase (*GAPDH*) was used as a reference for normalization. Each sample was tested three times, and samples from three independent experiments were used for analysis. The relative level of gene expression was calculated using the 2<sup>- $\Delta\Delta$ Ct</sup> method.<sup>35</sup>

### E. Western blot analysis

After plasma treatment, cells were cultured for 2, 4, or 6 days and then harvested in lysis buffer (Beyotime, Jiangsu, China) with

TABLE I. Primer sequences for qRT-PCR.

Gene	Primer sequence	Length (bp)
<i>Nestin</i>	5'-GGGTCTACAGAGTCAGATCGCTCA-3' 5'-AGCGAGAGTTCTCAGCCTCCA-3'	122
<i>β-Tubulin III</i>	5'-ACCTATTCAGGCCCGACAACCTTA-3' 5'-GCAGGCAGTCACAATTCTCACAC-3'	144
<i>GAPDH</i> (NM_008084.2)	5'-TGTGTCCGTCGTGGATCTGA-3' 5'-TTGCTGTTGAAGTCGCAGGAG-3'	150
<i>Notch1</i> (NM_008714.3)	5'-ATGCTGCTGTTGTGCTCCTGA-3' 5'-ATCCGTGATGTCCCGGTTG-3'	149
<i>Id2</i> (NM_010496.3)	5'-ATGAAAGCCTTCAG TCCGGTG-3' 5'-AGCAGACTCATCGGGTCGT-3'	144
<i>Ascl1</i> (NM_008553.4)	5'-AAGAGCTGCTGGACTTTACCAACTG-3 5'-ATTTGACGTGCTTGGCGAGA-3'	122
<i>Ngn2</i> (NM_009718.2)	5'-CCCAGATTCGTCACAATGCCTA-3' 5'-ACGCTTGCATTCAACCCTTACA-3'	168
<i>NeuroD</i> (U28068.1)	5'-CAGGGTTATGAGATCGTC-3' 5'-GTTTCTGGGTCTTGGAGT-3'	131

the protease inhibitor phenylmethanesulfonyl fluoride (PMSF, Beyotime, Jiangsu, China). The proteins in each sample were then separated by sodium dodecyl sulfate–polyacrylamide gel electrophoresis (SDS-PAGE), with  $\sim 30 \mu\text{g}$  of total cellular proteins being loaded per lane. The separated proteins were then transferred onto a nitrocellulose membrane, which was incubated with antibodies against iNOS (Santa Cruz, CA), Notch1 (Abcam, Cambridge, MA), Id2 (Abcam), Ngn2 (Santa Cruz), Ascl1 (Abcam), NeuroD (Santa Cruz), and  $\beta$ -actin (Santa Cruz) after blocking with 5% nonfat dried milk. HRP-conjugated goat anti-mouse or goat anti-rabbit IgG was used to detect the primary antibodies above. The detection of transferred proteins (antigens) was performed with an enhanced chemiluminescence detection kit (Millipore, USA) using the ChemiDoc XRS+ system (Bio-Rad, USA).

### F. Nitric oxide detection

Extracellular and intracellular aqueous NO concentrations were determined using an NO detection kit (Beyotime, Jiangsu, China) according to the manufacturer's instructions. For determination of extracellular NO, the conditioned medium from C17.2-NSC cultures immediately after plasma treatment and after a further 2, 4, or 6 days' incubation was collected as test samples. For determination of the intracellular NO concentration, cells were washed twice with ice-cold PBS and were then lysed using cell lysis buffer (Beyotime, Jiangsu, China) at the same time point described above. The lysates were collected and centrifuged for 5 min at 4 °C. The supernatants were then used as samples for testing.

### G. Statistical analysis

The morphology analysis and the percentage of  $\beta$ -Tubulin III-positive cells over the total number of cells (labeled with Hoechst) were determined for a minimum of 10 randomly selected fields by using Image-Pro Plus software. GraphPad Prism 7 software was used for statistical analysis. Results were expressed as the

mean  $\pm$  standard error of the mean (SEM), and reproducibility was confirmed in at least three independent experiments. Paired *t*-test and two-way ANOVA were used to assess statistical differences between groups. \* represents  $p < 0.05$ ; \*\* represents  $p < 0.01$ .

## III . RESULTS

Plasma pretests were carried out to determine the optimum plasma dosage used in the differentiation experiments. WST-1 method was used to evaluate the effects of different plasma doses (0, 5 s, 15 s, 30 s, 60 s, and 90 s) on the proliferation of C17.2 NSCs in 96-well plates. As can be seen from Fig. S1 in the [supplementary material](#), low-dose plasma treatment (plasma treatment for 5 s and 15 s) basically does not inhibit the proliferation of C17.2 NSCs, and, to a certain extent, plasma can promote the proliferation of C17.2 cells (48 h detection); however, high-dose plasma treatment (plasma treatment for 60 s and 90 s) has an obvious inhibitory effect on C17.2 proliferation, which is unfavorable to the *in vitro* differentiation of neural stem cells.

Since the WST-1 experiment used a 96-well plate with an area of  $0.37 \text{ cm}^2$  per well; however, the subsequent differentiation experiment used 12-well plates with an area of  $3.8 \text{ cm}^2$  per well, which was about 10 times the area of 96-well plates. Therefore, the energy density of plasma that  $<15 \text{ s}$  per well of 96-well plates and  $<150 \text{ s}$  per well of 12-well plates were considered to have no cytotoxic effect on C17.2 NSCs and could be used to study the effect of plasma on the differentiation of C17.2 NSCs. To determine the optimum plasma dosage used in the differentiation experiments in 12-well plates, different plasma dosages of 30 s, 45 s, 60 s, and 90 s were used and the general cell morphologies were recorded by the inverted phase contrast microscope on the 2nd, 4th, and 6th day after plasma treatment. As shown in Fig. S2 in the [supplementary material](#), 60 s plasma treatment can effectively induce the differentiation of C17.2 NSCs, while 90 s plasma treatment will cause cell shedding with a large area. Thus, 60 s plasma treatment was the



optimum plasma dosage and was used in the subsequent differentiation experiment.

Figure 2 shows the general cell morphology recorded by the inverted phase contrast microscope on the 2nd, 4th, and 6th day after plasma treatment. While being maintained in the differentiation medium, the C17.2 NSCs in each group gradually differentiated into nerve cells. However, at a given incubation time, accelerated cell differentiation was observed in the 60 s plasma-treated group, with much greater numbers of neurites and cell body extensions. There were no significant changes in cell morphology between the untreated control group and the 60 s gas flow control group. More specifically, a neural network started to form in the 60 s plasma-treated group after incubation in differentiation medium for 6 days, which was rarely seen in the other two groups.

Figure 3 shows immunofluorescence images of neurons after 6 days' incubation in all three groups. Nuclei were stained with blue dye (Hoechst 33258), and red ( $\beta$ -Tubulin III +) represents neurites in neuron cells. There is further confirmation here that atmospheric plasma jet treatment can enhance the differentiation of C17.2 NSC into neurons. For direct comparison, Table II presents the differentiation ratio, neurite length, and number of branching dendrites in both the control group and the 60 s plasma-treated group. The ratio of  $\beta$ -Tubulin III-positive cells is much greater in the plasma-treated group:  $77.23 \pm 3.06$ , compared with  $31.87 \pm 2.37$  in the control group ( $p = 0.007$ ,  $p < 0.01$ ). The neurons are more mature in the plasma-treated group, with elongated neurites of  $275.6 \pm 31.44 \mu\text{m}$  compared with  $156.6 \pm 13.13 \mu\text{m}$  in the control group ( $p = 0.006$ ,  $p < 0.01$ ). The average number of primary dendrites is also greater in the plasma-treated group:  $3.47 \pm 0.39$  compared with  $2.00 \pm 0.169$  in the control group ( $p = 0.002$ ,  $p < 0.01$ ).

Quantitative PCR and immunoblotting assays were used to measure the expression of specific genes after plasma treatment. *Nestin* and  $\beta$ -Tubulin III genes after 2, 4, and 6 days' incubation were quantified by qRT-PCR. *Nestin* has been reported to be expressed in undifferentiated neural cells and  $\beta$ -Tubulin III to be expressed only in neurons.<sup>36,37</sup> The results shown in Fig. 4 demonstrate that plasma exposure downregulated the expression of *Nestin* and upregulated that of  $\beta$ -Tubulin III in a plasma dose-dependent manner. The relative *Nestin* gene expression in the 60 s plasma-treated group decreased from 1.0 to 0.6 on the 2nd day and from 0.8 to 0.15 on the 6th day, compared with the control group. In contrast to *Nestin* expression,  $\beta$ -Tubulin III expression increased with plasma treatment time and it was  $\sim 2$  times higher in the 60 s plasma-treated group than that of control ( $p < 0.01$ ). We also compared the expressions of biomarkers in the control group and the gas flow control group and no significant differences were found between the two groups (see Fig. S3 in the supplementary material). These results indicated that the gene expression profiles were changed in a plasma dose-dependent manner, and the downregulation of *Nestin* and upregulation of  $\beta$ -Tubulin III led to the promoted neuronal differentiation.

Changes in the related transcription factors were also detected by qRT-PCR. As can be seen in Fig. 5, *Notch1* was downregulated in the plasma-treated group in a plasma dose-dependent manner, while *Ngn2* and *Ascl1* were upregulated. *Id2*, encoding an inhibitory protein in the bHLH family, was upregulated with prolonged incubation time. However, the expression of *Id2* in 45 s and 60 s plasma-treated groups were significantly lower than that in the untreated control group at the same time point. This may be due to the regulation of neuronal differentiation balance. The relative expression of *NeuroD*, which showed no significant difference among groups on

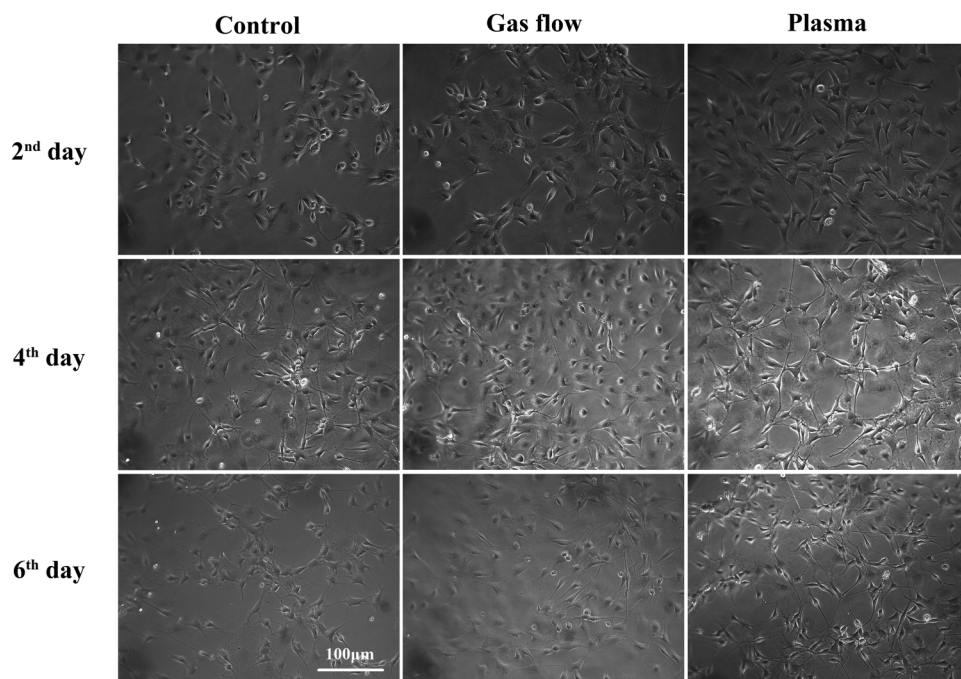
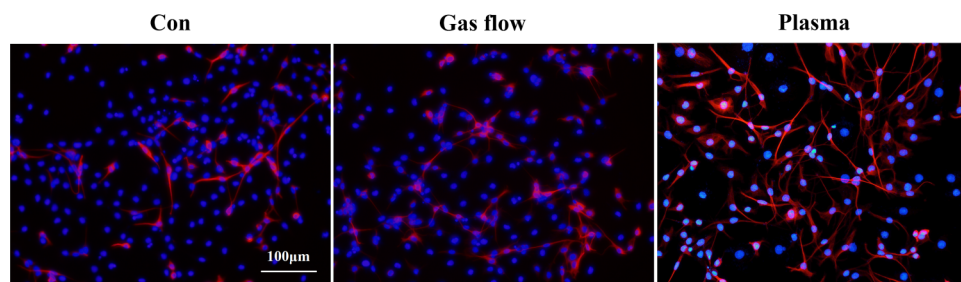


FIG. 2. Comparison of C17.2 NSCs differentiation in control, gas flow, and 60-s plasma-treatment groups by the inverted phase contrast light microscope images on the 2nd, 4th, and 6th days.



**FIG. 3.** Immunofluorescence images for identification of neuronal fate. The red biomarker ( $\beta$ -Tubulin III) represents axon-growth-specific expression in neurons. The nuclei were labeled by Hoechst 33258 (blue).

the 2nd day and 4th day, was greatly increased on the 6th day (by  $\sim 4$  times compared with the control group) in a plasma dose-dependent manner. This indicated that *NeuroD* was a relatively downstream transcription factor and plasma treatment enhanced its transcriptional activity. However, the expression of signaling factors in the gas flow group showed no statistical differences to that of the control group (Fig. S3 in the [supplementary material](#)). The results for transcription factor expression demonstrate that plasma treatment inhibited the *Notch1* signaling, downregulated the expression of *Id2*, and enhanced the expression of *Ngn2* and *Ascl1*, thereby initiating neuronal differentiation and activating the downstream differentiation factor *NeuroD*.

The expressions of related proteins in neuronal differentiation were also detected by western blot analysis. The expression trends of signaling proteins are consistent with the expressions of the corresponding genes, as can be seen in Fig. 6.

To investigate the mechanism of plasma-induced neuronal differentiation, changes in extracellular and intracellular NO concentrations during incubation were measured (Fig. 7). The immediate NO concentration in the cell culture medium after 60 s plasma treatment reached  $\sim 85$  nmol/ml, whereas only  $\sim 2$  nmol/ml was detected in the control and gas flow groups. The immediate intracellular NO concentration was close to zero in all three groups. The extracellular NO concentrations in the control and gas flow groups increased slightly, with values ranging from 2 to 10 nmol/ml after 6 days' incubation. Due to the replacement of plasma-treated medium, the extracellular NO concentration in the 60 s plasma-treated group decreased remarkably on the 2nd day (10 nmol/ml), but it increased significantly on the 4th day (25 nmol/ml) as well as on the 6th day (30 nmol/ml), compared with control and gas flow groups. The intracellular NO concentration for the 60 s plasma treatment was as high as twice that of the control and gas flow groups on the 2nd and 4th days. It should be noted here that the

cell culture medium was changed every other day, so the extracellular NO on the 2nd, 4th, and 6th day must have originated from diffusion of intracellular NO into the cell culture medium as a result of metabolic processes. These results indicate that plasma treatment can induce increases in both extracellular and intracellular NO, which may be critical for the accelerated neuronal differentiation process.

We also measured iNOS expression by western blot analysis. iNOS is an intracellular NO synthase that regulates NO formation. Figure 8 shows the expression of intracellular iNOS, which could indirectly reflect the level of NO in cells. iNOS expression was much higher in the plasma-treated group and increased with incubation time. This is consistent with the intracellular NO measurement in Fig. 7 and confirms that plasma treatment induced intracellular NO synthesis by upregulating iNOS expression.

#### IV. DISCUSSION

Although applications of CAPs in biomedicine have been investigated for many years, research on their use to enhance stem cell differentiation is still in its early stages. There have been only a few reports on such work, especially with regard to NSC differentiation.<sup>38–41</sup> Moreover, the mechanisms involved in the CAP interactions with microorganisms and living tissues or *in vivo* are far from understood. In this study, we investigated the mechanisms underlying enhancement of NSC differentiation by CAPs, specifically the role of NO generated by an atmospheric He/O<sub>2</sub> plasma jet in the accelerated differentiation process. We found that 60 s He/O<sub>2</sub> plasma jet treatment can effectively enhance the differentiation of C17.2 NSCs. To follow the course of neuron formation, we used an exclusive biomarker,  $\beta$ -Tubulin III, which is a cell cytoskeletal protein that is expressed during axonal outgrowth.<sup>42</sup> Immunofluorescence results clearly showed that  $77.23 \pm 3.06\%$  cells were  $\beta$ -Tubulin III-positive

**TABLE II.** Comparison of differentiation ratio, neurite length, and number of branching dendrites in the control and 60 s plasma-treated groups.

	Control	60 s plasma-treated	<i>t</i> -test
$\beta$ -Tubulin III-positive cells (100%) (mean $\pm$ SEM)	$31.87 \pm 2.37$ ( <i>n</i> = 12)	$77.23 \pm 3.06$ ( <i>n</i> = 12)	<i>p</i> = 0.007 ( <i>p</i> < 0.01)
Neurite length ( $\mu$ m) (mean $\pm$ SEM)	$156.60 \pm 13.13$ ( <i>n</i> = 120)	$275.60 \pm 31.44$ ( <i>n</i> = 120)	<i>p</i> = 0.006 ( <i>p</i> < 0.01)
Number of branching dendrites (mean $\pm$ SEM)	$2.00 \pm 0.169$ ( <i>n</i> = 120)	$3.47 \pm 0.39$ ( <i>n</i> = 120)	<i>p</i> = 0.002 ( <i>p</i> < 0.01)

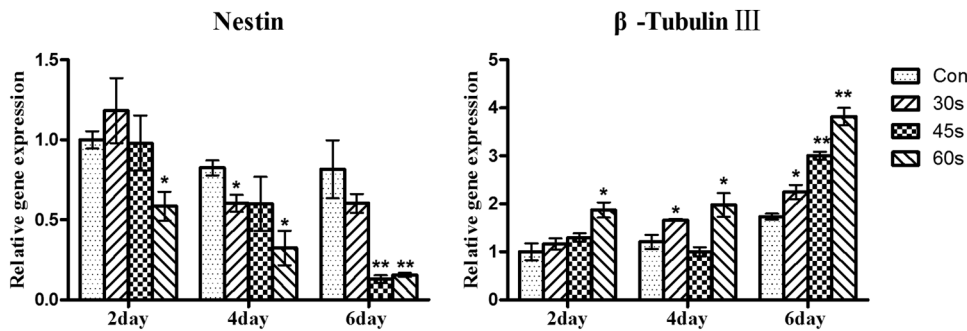


**FIG. 4.** qRT-PCR analysis showing the effect of plasma treatment on expressions of *Nestin* and *β-Tubulin III*. Expression change (-fold) for individual genes was obtained by comparing the gene expression in plasma-treated groups with that of control on the 2nd day. Each column represents the mean ± SEM of three independent experiments. \* $p < 0.05$ ; \*\* $p < 0.01$ . The  $p$  values were obtained by a two-way ANOVA.

(stained red, neurons) and showed more mature cell morphology, with larger cell bodies, increased number of dendrites, and greater neurite length, in the plasma-treated group.

There may be various precipitating factors generated by the He/O<sub>2</sub> plasma jet that are involved in this phenomenon, such as short-lived species, heat, ultraviolet (UV) radiation, and electric fields, among which reactive oxygen and nitrogen species (RONS) are thought to be the key factor in many interactions.<sup>43,44</sup> Many short-lived radicals, excited-state particles, and metastable-state atoms have significant roles in physical and chemical kinetic processes and may also be involved in the interactions of the plasma when it comes into direct contact with other entities.<sup>45</sup> However in this case, during the plasma treatment, the NSCs seeded in

12-well plates were covered with 800 μl cell culture medium, and therefore these short-lived species could not come into direct contact with the cells.

No significant differences were observed between the control and gas flow groups, indicating that gas flow alone has no effect on C17.2 NSC differentiation. The measured gas temperature of the pulsed DC power driven He/O<sub>2</sub> plasma jet was ~300 K (close to room temperature),<sup>34</sup> and so thermal effects could also be excluded.

The power consumption of the He/O<sub>2</sub> plasma was less than 1 W, and the UV radiation produced was of the order of milliwatts.<sup>46</sup> Wong *et al.*<sup>47</sup> found that low-dose, long-wave UV light does not affect gene expression of human mesenchymal stem cells. Besides, the liquid layer would have prevented the UV radiation from reach

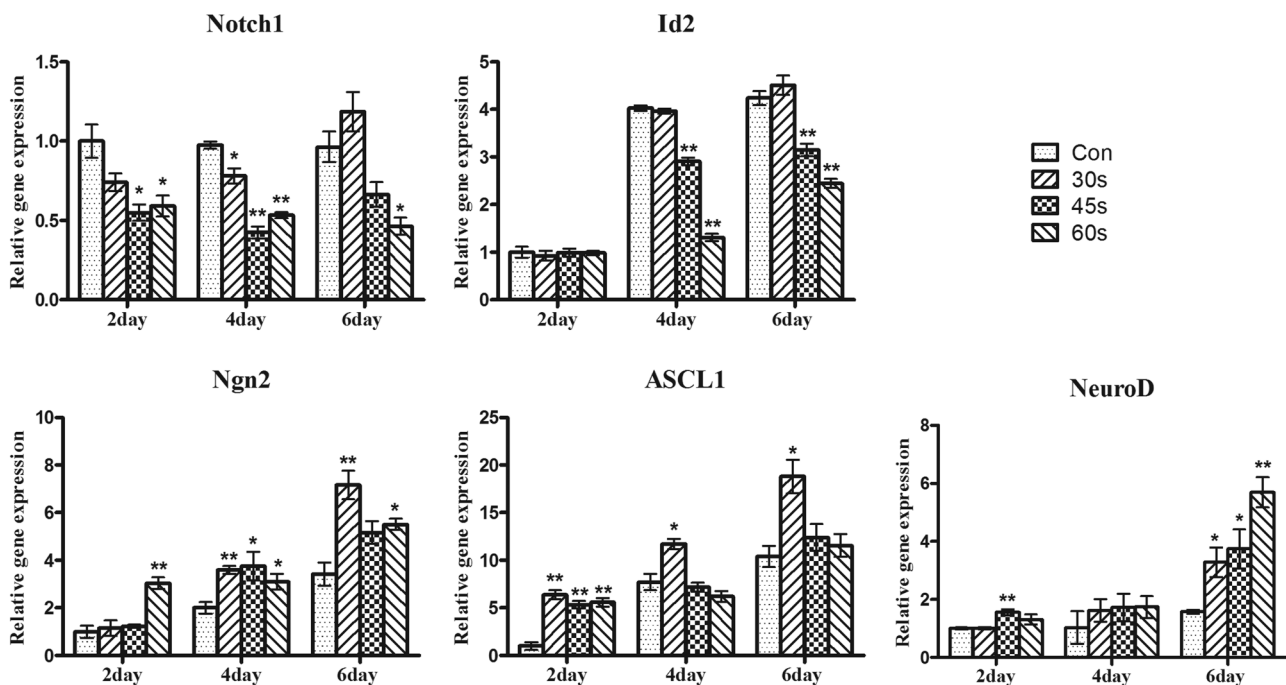


**FIG. 5.** qRT-PCR analysis showing the effect of plasma treatment on expressions of neuronal-differentiation-related genes. Expression change (-fold) for individual genes was obtained by comparing the gene expression in plasma-treated groups with that of control on the 2nd day. Each column represents the mean ± SEM of three independent experiments. \* $p < 0.05$ ; \*\* $p < 0.01$ . The  $p$  values were obtained by a two-way ANOVA.



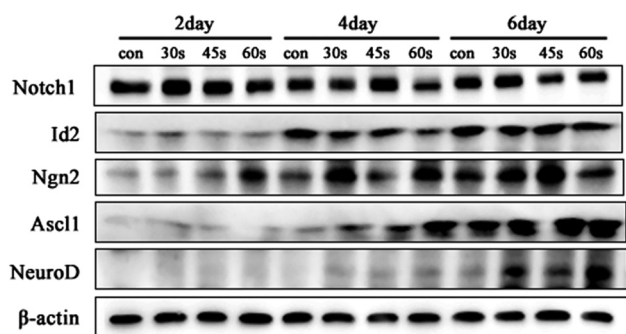


FIG. 6. Effects of plasma treatment on the expression of neuronal differentiation-related proteins.

the NSCs directly. Hence, it can be assumed that UV radiation did not make a significant contribution to the differentiation process in this study.

Pulsed DC electric fields with particular characteristics may have a variety of effects on NSCs differentiation. Chang *et al.*<sup>48</sup> reported that a 300 mV/mm 100 Hz square-wave DC pulse could induce differentiation of cortical neural precursor cells with stimulation times of up to 48 h. Kobelt *et al.*<sup>49</sup> found that two days of treatment at 10 min/day with 0.53 V/m DC stimulation increased the length of neural stem progenitor cells by a factor of more than five compared with controls. These investigations used relatively long treatment times and low electric fields of strengths, which is close to those of endogenous electrical fields in the central nervous system, whereas in the experiments described here, the electric field strength along the plasma plume was in the range of 9–17 kV/cm (Ref. 50) and the treatment time was only several tens of seconds. Such a high electrical field may induce cancer cell apoptosis instead of differentiation,<sup>51</sup> and we also found cell death in the center of the treatment area where the plasma plume directly contacted the liquid surface.

As reported in our previous work and elsewhere,<sup>32,33</sup> NO generated by CAPs may have a key effect on NSCs differentiation. We used SNP as an exogenous NO donor with a similar aqueous concentration as the plasma jet created in the cell culture medium. In the positive control group, exogenous NO with a similar concentration

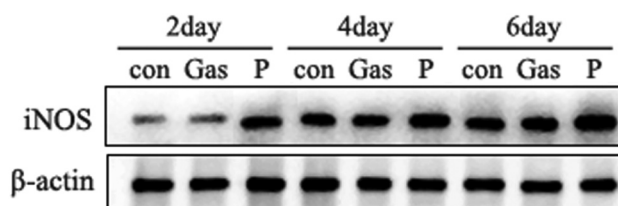


FIG. 8. Intracellular iNOS expression by western blot analysis.

yielded almost the same neuronal differentiation ratio. Moreover, in the negative control group, in which the NO scavenger Hgb was added to the cell culture medium before plasma treatment, there was nearly no difference in NSCs differentiation compared with the control (no treatment) group, which indicated that the NO scavenger compromised the effect of the plasma treatment. Therefore, the electric field and other long-lived species in the plasma are not important factors in the process investigated here. Hence, we focused on the mechanism of accelerated and directed neuronal differentiation induced by NO from the plasma jet.

Recent research has shown that NO participates in the regulation of synaptic transmission and neurotransmitter release and that exogenous NO could affect NSCs proliferation and differentiation.<sup>52,53</sup> Arnhold *et al.*<sup>54</sup> found that exogenous NO could significantly enhance the differentiation of NSCs into neurons and accelerate axon growth and that lack of NO led to inhibition of axon growth. Nevertheless, there was NO dose dependence in the regulation of NSCs differentiation. Covacu *et al.*<sup>55</sup> found that 500 nM NO exposure changed the differentiation fate of NSCs from neurons to glias. Meanwhile, cell viability is also related to plasma dosage, which in our case mainly refers to plasma-treatment time. We performed various pretests to determine the proper plasma treatment time. Very short treatment had no significant effect on NSC differentiation. Treatment for less than 15 s (in 96-well plates) would enhance cell proliferation, but more than 90 s treatment (in 96-well plates) would severely decrease cell viability (Fig. S1 in the supplementary material). With a plasma-treatment time of less than 60 s (in 12-well plates), the NSCs exhibited obvious differentiation and no significant cell death. The 60 s plasma treatment created

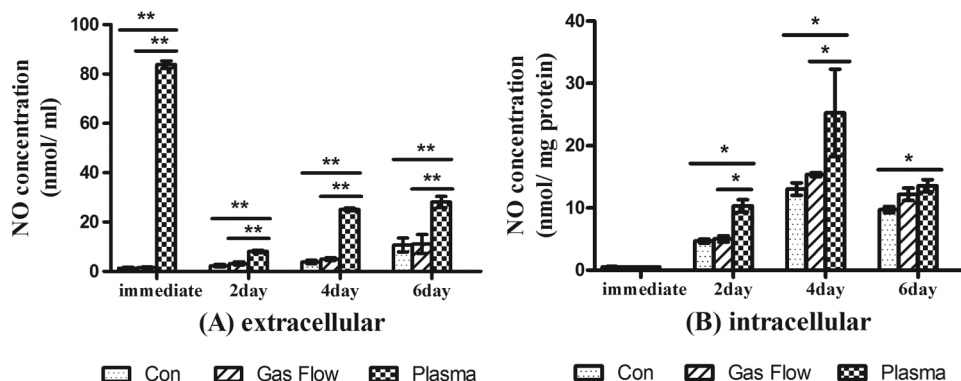
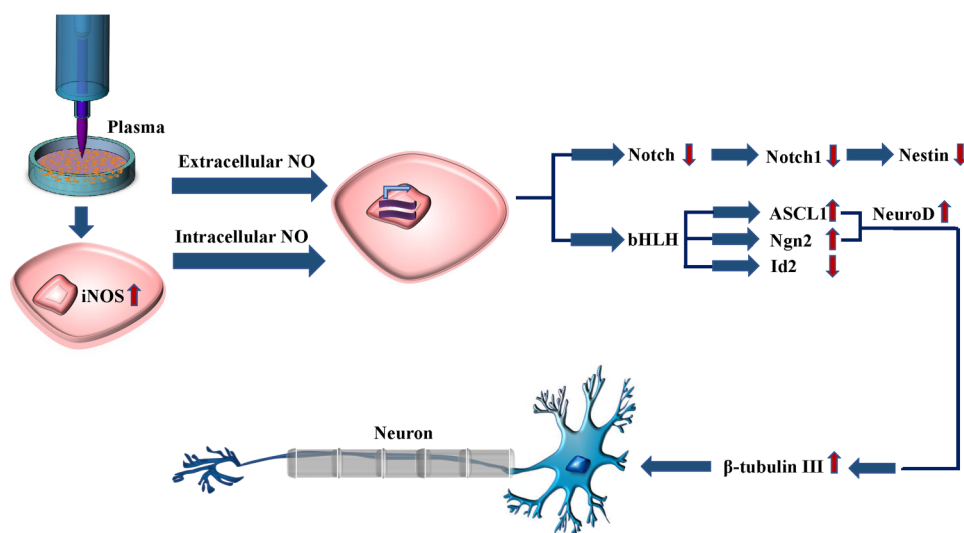


FIG. 7. Extracellular (a) and intracellular (b) NO concentration detection as functions of incubation time. Each column represents the mean  $\pm$  SEM of three independent experiments. \* $p < 0.05$ ; \*\* $p < 0.01$ . The  $p$  values were obtained by a two-way ANOVA.



**FIG. 9.** Summary of the mechanism of enhanced neuronal differentiation by plasma treatment.

~85 nmol/ml NO in the cell culture medium [immediate measurement, Fig. 7(a)], which is within the physiological NO concentration of 10–100 nmol/ml in the brain, and would benefit neuronal differentiation. The extracellular NO concentration in the plasma-treated group on different days showed significant differences compared with the control group ( $p < 0.01$ ). As mentioned above, the cell culture medium was replaced with fresh medium 1 h after plasma treatment and then again every other day. Therefore, the NO detected in the culture medium on the 2nd, 4th, and 6th days must have been synthesized internally by the cells and then diffused out.

The intracellular NO concentration was significantly larger in the plasma-treatment group than that in the control group: by a factor of almost 2 times on the 2nd day [Fig. 7(b)] ( $p < 0.05$ ). There was a large fluctuation in the intracellular NO concentration in the plasma-treated group on the 4th day, which may be caused by individual differences among the samples. The immediate intracellular NO concentration was close to zero, which indicated that the increase in intracellular NO during incubation was not due to diffusion of exogenous NO into the cell, but rather to internal NO synthesis. Arnhold *et al.*<sup>54</sup> pointed out that the expression of the synthase iNOS in NSCs and the consequent synthesis of intracellular NO are the key factors in changing the proliferation of NSCs into a differentiation process. In the present study, iNOS expression increased after plasma treatment, as shown in Fig. 8. Therefore, we can conclude that plasma treatment activated the expression of iNOS, leading to the intracellular formation of NO, which played a critical role in the differentiation process.

NO is also reported to regulate gene expression in several ways<sup>51</sup> and can regulate the expression of some transcriptional genes involved in cellular survival and neurogenesis.<sup>52</sup> Notch and the bHLH family are considered to be the most important transcription factors in neural differentiation and regeneration processes. Notch1 is expressed mainly in undifferentiated neural stem cells and maintains the undifferentiated status.<sup>56</sup> The bHLH family participates mainly in the regulation of neuronal differentiation,<sup>9</sup> in which *Ascl1* and *Ngn2* are responsible for activation of neuronal

generation.<sup>57,58</sup> *Ngn2* is the transcriptional initiator of *NeuroD*, and its main function is activating downstream *NeuroD* and initiating neuron differentiation. Meanwhile, *NeuroD* is the main differentiation factor.<sup>59</sup> The bHLH family also includes negative transcription factors such as *Id2*, which usually inhibits the differentiation of neurons to maintain a balance. From the present results, it can be seen that the trends of *Nestin* and  $\beta$ -*Tubulin III* gene expression (Fig. 4) were the same as those of *Notch1*, *Ngn2*, and *NeuroD* (Figs. 5 and 6), which regularly increased with increasing NO concentrations. In the plasma-treated group, the expression of *Ascl1* showed a significant difference from that in the control group on the 2nd day, while *Id2* expression decreased on the 4th and 6th days. We are not at present able to give an exact explanation for the relationship between the expression of these genes and the NSC differentiation process. However, from the existing results, we can give a reasonable summary of the mechanism underlying the accelerated and directed neuronal differentiation of C17.2 NSCs by an atmospheric He/O<sub>2</sub> plasma: see Fig. 9. On the one hand, the plasma jet creates gaseous NO, which diffuses into the cell culture medium, playing the role of an exogenous NO donor; on the other hand, the plasma treatment stimulates iNOS expression in the cells, leading to the synthesis of intracellular NO. Both extracellular and intercellular NO then regulate the transcriptional activity of genes involved in neurogenesis, with *Notch1* and *Id2* expression being downregulated, and *Ascl1* and *Ngn2* expression upregulated, finally leading to upregulation of downstream *NeuroD*, causing NSC differentiation into neurons.

Plasma treatment thus represents a promising approach, offering a one-step, effective and fast way to achieving directed NSC differentiation *in vitro* compared with traditional methods. However, there are some challenges during the experiments. It was necessary to perform pretests to determine the proper plasma dosage, which needed a lot of work on plasma diagnostics. In the context of plasma treatment, the gas flow from the plasma jet device comes into direct contact with the sample, which could cause nonuniformity in the cell wall. An inwardly directed treatment mode or the use of a plasma

active medium might help to eliminate this disadvantage and may allow bulk processing in the future. For the study of the mechanisms involved on the gene level, we focused on the relationships between the expressions of a number of genes and neuronal differentiation, ignoring other possible genes or signaling pathways, which therefore remain to be studied in future work.

## V. CONCLUSION

We have investigated the mechanism of enhanced and directed neuronal differentiation of C17.2 NSCs induced by an atmospheric He/O<sub>2</sub> plasma jet. The exogenous NO in the plasma and the increased intracellular NO synthesized by iNOS after plasma stimulation are the key factors for directed neuronal differentiation, by downregulating the expression of *Notch1* and upregulating those of *Ascl1* and *Ng2* to activate downstream *NeuroD*, which regulates the differentiation of NSCs into neurons.

## SUPPLEMENTARY MATERIAL

See the [supplementary material](#) for the plasma dosage pretest of cell viability and differentiation as well as the comparison of biomarkers and signaling factors expression in the control group and the gas flow control group.

## ACKNOWLEDGMENTS

The authors are grateful for financial support from the Huazhong Scholar Program, the Independent Innovation Fund of Huazhong University of Science and Technology (No. 2018KFYXJ071), and the National Natural Science Foundation of China (NNSFC) (No. 31501099).

## REFERENCES

- <sup>1</sup>J. J. Sejvar, *Lancet Neurol.* **16**, 858 (2017).
- <sup>2</sup>V. L. Feigin, A. A. Abajobir, K. H. Abate, F. Abd-Allah, A. M. Abdulle, S. F. Abera, G. Y. Abyu, M. B. Ahmed, A. N. Aichour, I. Aichour, M. T. E. Aichour, R. O. Akinyemi, S. Alabed, R. Al-Raddadi, N. Alvis-Guzman, A. T. Amare, H. Ansari, P. Anwari, J. Ärnlöv, H. Asayesh, S. W. Asgedom, T. M. Atey, L. Avila-Burgos, E. Frinel, G. A. Avokpaho, M. R. Azarpazhooh, A. Barac, M. Barboza, S. L. Barker-Collo, T. Barnighausen, N. Bedi, E. Beghi, D. A. Bennett, I. M. Bensenor, A. Berhane, B. D. Betsu, S. Bhaumik, S. M. Birlık, S. Biryukov, D. J. Boneya, L. N. B. Bulto, H. Carabin, D. Casey, C. A. Castañeda-Orjuela, F. Catalá-López, H. Chen, A. A. Chitheer, R. Chowdhury, H. Christensen, L. Dandona *et al.*, *Lancet Neurol.* **16**, 877 (2017).
- <sup>3</sup>L. A. Flanagan, L. M. Rebaza, S. Derzic, P. H. Schwartz, and E. S. Monuki, *J. Neurosci. Res.* **83**, 845 (2006).
- <sup>4</sup>T. R. Ham, M. Farrag, and N. D. Leipzig, *Acta Biomater.* **53**, 140 (2017).
- <sup>5</sup>M. Bani-Yaghoob, S. E. Kendall, D. P. Moore, S. Bellum, R. A. Cowling, G. N. Nikopoulos, C. J. Kubu, C. Vary, and J. M. Verdi, *Development* **131**, 4287 (2004).
- <sup>6</sup>F. Huang, Q. Shen, and J. Zhao, *Neural Regen. Res.* **8**, 313 (2013).
- <sup>7</sup>F. Pires, Q. Ferreira, C. A. V. Rodrigues, J. Morgado, and F. C. Ferreira, *Biochim. Biophys. Acta Gen. Subj.* **1850**, 1158 (2015).
- <sup>8</sup>R. A. Barker, J. Drouin-Ouellet, and M. Parmar, *Nat. Rev. Neurol.* **11**, 492 (2015).
- <sup>9</sup>E. Navarro Quiroz, R. Navarro Quiroz, M. Ahmad, L. Gomez Escorcía, J. Villarreal, C. Fernandez Ponce, and G. Aroca Martinez, *Cells* **7**, 75 (2018).
- <sup>10</sup>Y. Shi, D. Chichung Lie, P. Taupin, K. Nakashima, J. Ray, R. T. Yu, F. H. Gage, and R. M. Evans, *Nature* **427**, 78 (2004).
- <sup>11</sup>M. Bylund, E. Andersson, B. G. Novitsch, and J. Muhr, *Nat. Neurosci.* **6**, 1162 (2003).
- <sup>12</sup>R. Kageyama, T. Ohtsuka, J. Hatakeyama, and R. Ohsawa, *Exp. Cell Res.* **306**, 343 (2005).
- <sup>13</sup>A. Alvarez-Buylla and D. A. Lim, *Neuron* **41**, 683 (2004).
- <sup>14</sup>H. Ding, K. C. Keller, I. K. C. Martinez, R. M. Geransar, K. O. zur Nieden, S. G. Nishikawa, D. E. Rancourt, and N. I. zur Nieden, *J. Cell Sci.* **125**, 5564 (2012).
- <sup>15</sup>R. Zhang, L. Zhang, Z. Zhang, Y. Wang, M. Lu, M. LaPointe, and M. Chopp, *Ann. Neurol.* **50**, 602 (2001).
- <sup>16</sup>N. Peunova and G. Enikolopov, *Nature* **364**, 450 (1993).
- <sup>17</sup>J. L. Franklin and E. M. Johnson, *Trends Neurosci.* **15**, 501 (1992).
- <sup>18</sup>M. Laroussi, X. Lu, and M. Keidar, *J. Appl. Phys.* **122**, 020901 (2017).
- <sup>19</sup>G. J. Lee, M. A. Choi, D. Kim, J. Y. Kim, B. Ghimire, E. H. Choi, and S. H. Kim, *J. Appl. Phys.* **122**, 103303 (2017).
- <sup>20</sup>B. Haertel, T. von Woedtke, K.-D. Weltmann, and U. Lindequist, *Biomol. Ther. (Seoul)* **22**, 477 (2014).
- <sup>21</sup>K.-D. Weltmann and T. von Woedtke, *Plasma Phys. Control. Fusion* **59**, 014031 (2017).
- <sup>22</sup>D. B. Graves, *Phys. Plasma* **21**, 080901 (2014).
- <sup>23</sup>M.-H. T. Ngo, J.-D. Liao, P.-L. Shao, C.-C. Weng, and C.-Y. Chang, *Plasma Process. Polym.* **11**, 80 (2014).
- <sup>24</sup>M. Keidar, *Plasma Sources Sci. Technol.* **24**, 033001 (2015).
- <sup>25</sup>S. Bekechus, A. Schmidt, K.-D. Weltmann, and T. von Woedtke, *Clin. Plasma Med.* **4**, 19 (2016).
- <sup>26</sup>G. Isbary, G. Morfill, J. Zimmermann, T. Shimizu, and W. Stolz, *Arch. Dermatol.* **147**, 388 (2011).
- <sup>27</sup>G. Isbary, W. Stolz, T. Shimizu, R. Monetti, W. Bunk, H.-U. Schmidt, G. E. Morfill, T. G. Klämpfl, B. Steffes, H. M. Thomas, J. Heinlin, S. Karrer, M. Landthaler, and J. L. Zimmermann, *Clin. Plasma Med.* **1**, 25 (2013).
- <sup>28</sup>J. Heinlin, G. Isbary, W. Stolz, G. Morfill, M. Landthaler, T. Shimizu, B. Steffes, T. Nosenko, J. Zimmermann, and S. Karrer, *J. Eur. Acad. Dermatol. Venerol.* **25**, 1 (2011).
- <sup>29</sup>M. J. Pavlovich, D. S. Clark, and D. B. Graves, *Plasma Sources Sci. Technol.* **23**, 065036 (2014).
- <sup>30</sup>C. Douat, S. Hübner, R. Engeln, and J. Benedikt, *Plasma Sources Sci. Technol.* **25**, 025027 (2016).
- <sup>31</sup>A. V. Pipa, S. Reuter, R. Foest, and K.-D. Weltmann, *J. Phys. D Appl. Phys.* **45**, 085201 (2012).
- <sup>32</sup>Z. Xiong, S. Zhao, X. Mao, X. Lu, G. He, G. Yang, M. Chen, M. Ishaq, and K. Ostrikov, *Stem Cell Res.* **12**, 387 (2014).
- <sup>33</sup>J.-Y. Jang, Y. J. Hong, J. Lim, J. S. Choi, E. H. Choi, S. Kang, and H. Rhim, *Biomaterials* **156**, 258 (2018).
- <sup>34</sup>X. Lu, Z. Jiang, Q. Xiong, Z. Tang, and Y. Pan, *Appl. Phys. Lett.* **92**, 151504 (2008).
- <sup>35</sup>U. Lendahl, L. B. Zimmerman, and R. D. G. McKay, *Cell* **60**, 585 (1990).
- <sup>36</sup>G. Kronenberg, K. Reuter, B. Steiner, M. D. Brandt, S. Jessberger, M. Yamaguchi, and G. Kempermann, *J. Comp. Neurol.* **467**, 455 (2003).
- <sup>37</sup>M. K. Lee, J. B. Tuttle, L. I. Rebbun, D. W. Cleveland, and A. Frankfurter, *Cell Motil. Cytoskeleton* **17**, 118 (1990).
- <sup>38</sup>M. Wang, X. Cheng, W. Zhu, B. Holmes, M. Keidar, and L. G. Zhang, *Tissue Eng. A* **20**, 1060 (2014).
- <sup>39</sup>W. Zhu, M. Keidar, and L. G. Zhang, *MRS Proc.* **1723**, mrsf14 (2014).
- <sup>40</sup>A. Ermakov, O. Ermakova, A. Skavulyak, N. Kreshchenko, S. Gudkov, and E. Maevsky, *Plasma Process. Polym.* **13**, 788 (2016).
- <sup>41</sup>A. Siu, O. Volotskova, X. Cheng, S. S. Khalsa, K. Bian, F. Murad, M. Keidar, and J. H. Sherman, *PLoS One* **10**, e0126313 (2015).
- <sup>42</sup>S. Zhao, Z. Xiong, X. Mao, D. Meng, Q. Lei, Y. Li, P. Deng, M. Chen, M. Tu, X. Lu, G. Yang, and G. He, *PLoS One* **8**, e73665 (2013).
- <sup>43</sup>A. Lin, N. Chernetz, J. Han, Y. Alicea, D. Dobrynin, G. Fridman, T. A. Freeman, A. Fridman, and V. Miller, *Plasma Process. Polym.* **12**, 1117 (2015).
- <sup>44</sup>D. B. Graves, *J. Phys. D Appl. Phys.* **45**, 263001 (2012).

- <sup>45</sup>C. A. J. van Gils, S. Hofmann, B. K. H. L. Boekema, R. Brandenburg, and P. J. Bruggeman, *J. Phys. D Appl. Phys.* **46**, 175203 (2013).
- <sup>46</sup>Q. Xiong, A. Y. Nikiforov, M. A. González, C. Leys, and X. P. Lu, *Plasma Sources Sci. Technol.* **22**, 015011 (2012).
- <sup>47</sup>D. Y. Wong, T. Ranganath, and A. M. Kasko, *PLoS One* **10**, e0139307 (2015).
- <sup>48</sup>H.-F. Chang, Y.-S. Lee, T. K. Tang, and J.-Y. Cheng, *PLoS One* **11**, e0158133 (2016).
- <sup>49</sup>L. J. Kobelt, A. E. Wilkinson, A. M. McCormick, R. K. Willits, and N. D. Leipzig, *Ann. Biomed. Eng.* **42**, 2164 (2014).
- <sup>50</sup>Y. Lu, S. Wu, W. Cheng, and X. Lu, *Eur. Phys. J. Spec. Top.* **226**, 2979 (2017).
- <sup>51</sup>H. B. Kim, S. Ahn, and S. B. Sim, in 30th International Conference on Plasma Science 2003, ICOPS 2003, IEEE Conference Record—Abstracts, p. 436.
- <sup>52</sup>A. Cheng, S. Wang, J. Cai, M. S. Rao, and M. P. Mattson, *Dev. Biol.* **258**, 319 (2003).
- <sup>53</sup>A. Park, H.-I. Lee, D. Semjid, D. K. Kim, and S.-W. Chun, *Neural Plast.* **2014**, 628531 (2014).
- <sup>54</sup>S. Arnhold, A. Faßbender, F.-J. Klinz, K. Kruttwig, B. Löhnig, C. Andressen, and K. Addicks, *Int. J. Dev. Neurosci.* **20**, 83 (2002).
- <sup>55</sup>R. Covacu, A. I. Danilov, B. S. Rasmussen, K. Hallén, M. C. Moe, A. Lobell, C. B. Johansson, M. A. Svensson, T. Olsson, and L. Brundin, *Stem Cells* **24**, 2792 (2006).
- <sup>56</sup>I. Imayoshi, M. Sakamoto, M. Yamaguchi, K. Mori, and R. Kageyama, *J. Neurosci.* **30**, 3489 (2010).
- <sup>57</sup>N. I. Park, P. Guilhamon, K. Desai, R. F. McAdam, E. Langille, M. O'Connor, X. Lan, H. Whetstone, F. J. Coutinho, R. J. Vanner, E. Ling, P. Prinos, L. Lee, H. Selvadurai, G. Atwal, M. Kushida, I. D. Clarke, V. Voisin, M. D. Cusimano, M. Bernstein, S. Das, G. Bader, C. H. Arrowsmith, S. Angers, X. Huang, M. Lupien, and P. B. Dirks, *Cell Stem Cell* **21**, 209 (2017).
- <sup>58</sup>S.-M. Ho, B. J. Hartley, J. Tcw, M. Beaumont, K. Stafford, P. A. Slesinger, and K. J. Brennand, *Methods* **101**, 113 (2016).
- <sup>59</sup>J. E. Lee, *Dev. Neurosci.* **19**, 27 (1997).